



Original Paper

Pore-scale probing CO₂ huff-n-puff in extracting shale oil from different types of pores using online T_1 – T_2 nuclear magnetic resonance spectroscopy



Yi-Jian Ren ^a, Bing Wei ^{a,*}, Bing-Xin Ji ^b, Wan-Fen Pu ^a, Dian-Lin Wang ^a, Jin-Yu Tang ^c, Jun Lu ^d

^a State Key Laboratory of Oil and Gas Reservoir Geology and Exploitation, Southwest Petroleum University, Chengdu, 610500, Sichuan, China

^b Tarim Oilfield, Korla, 842209, Xinjiang, China

^c Department of Chemical and Petroleum Engineering, United Arab Emirates University, Al Ain, Abu Dhabi, 15551, United Arab Emirates

^d McDougall School of Petroleum Engineering, The University of Tulsa, Tulsa, OK, 74104, USA

ARTICLE INFO

Article history:

Received 20 February 2024

Received in revised form

15 June 2024

Accepted 1 July 2024

Available online 2 July 2024

Edited by Yan-Hua Sun

Keywords:

Shale oil

Enhanced oil recovery

CO₂ huff-n-puff

Pore scale extraction

T_1 – T_2 NMR spectrum

ABSTRACT

CO₂ huff-n-puff shows great potential to promote shale oil recovery after primary depletion. However, the extracting process of shale oil residing in different types of pores induced by the injected CO₂ remains unclear. Moreover, how to saturate shale core samples with oil is still an experimental challenge, and needs a recommended procedure. These issues significantly impede probing CO₂ huff-n-puff in extracting shale oil as a means of enhanced oil recovery (EOR) processes. In this paper, the oil saturation process of shale core samples and their CO₂ extraction response with respect to pore types were investigated using online T_1 – T_2 nuclear magnetic resonance (NMR) spectroscopy. The results indicated that the oil saturation of shale core samples rapidly increased in the first 16 days under the conditions of 60 °C and 30 MPa and then tended to plateau. The maximum oil saturation could reach 46.2% after a vacuum and pressurization duration of 20 days. After saturation, three distinct regions were identified on the T_1 – T_2 NMR spectra of the shale core samples, corresponding to kerogen, organic pores (OPs), and inorganic pores (IPs), respectively. The oil trapped in IPs was the primary target for CO₂ huff-n-puff in shale with a maximum cumulative oil recovery (COR) of 70% original oil in place (OOIP) after three cycles, while the oil trapped in OPs and kerogen presented challenges for extraction (COR < 24.2% OOIP in OPs and almost none for kerogen). CO₂ preferentially extracted the accessible oil trapped in large IPs, while due to the tiny pores and strong affinity of oil-wet walls, the oil saturated in OPs mainly existed in an adsorbed state, leading to an insignificant COR. Furthermore, COR demonstrated a linear increasing tendency with soaking pressure, even when the pressure noticeably exceeded the minimum miscible pressure, implying that the formation of a miscible phase between CO₂ and oil was not the primary drive for CO₂ huff-n-puff in shale.

© 2024 The Authors. Publishing services by Elsevier B.V. on behalf of KeAi Communications Co. Ltd. This is an open access article under the CC BY-NC-ND license (<http://creativecommons.org/licenses/by-nc-nd/4.0/>).

1. Introduction

As conventional resources are depleting rapidly, the top priority is to secure the increasing global energy demand. Shale oil possesses abundant geological resources and could serve as a potential alternative to offset the decline of conventional resources. According to data from the US Energy Information Administration

(EIA), US shale oil production has shown a dramatical increase from 12% to over 62% of total crude oil production, indicating the significant potential of shale oil reservoirs (Chen et al., 2024). Due to the low permeability and porosity of shale matrix as well as the complex pore system, the development of shale reservoirs mainly depends on multistage hydraulic fracturing and horizontally placed wells, which usually yield an oil recovery of less than 8% original oil in place (OOIP), resulting in a significant volume of shale oil remaining trapped in the formation (Hoffman and Rutledge, 2019; Perez and Devegowda, 2020).

* Corresponding author.

E-mail address: bwei@swpu.edu.cn (B. Wei).

As an increase of a few percentage points in oil recovery could lead to millions of barrels of additional oil for a shale reservoir, effective enhanced oil recovery (EOR) methods become crucial in order to further promote the oil recovery and profitability of shale reservoirs. Gas huff-n-puff (cyclic injection) has proven to be a promising EOR process for shale oil recovery, among which CO₂ huff-n-puff has been widely investigated due to the significant interactions between CO₂ and oil, and the resulting re-pressurization, oil viscosity and interfacial tension (IFT) reduction through oil swelling, wettability alteration, light hydrocarbon vaporization, and relative permeability hysteresis (Fakher et al., 2020; Li et al., 2019). For example, Hawthorne et al. (2013, 2017) investigated the mechanisms of hydrocarbon mobilization from shale cores upon exposure to CO₂. It was found that a significant increase in oil recovery could be achieved by increasing soaking pressure to a magnitude beyond minimum miscible pressure (MMP), with solubility/diffusion being the dominant mechanism. Tovar et al. (2021) evaluated the efficiency of CO₂ EOR in shale and found that increasing pressure beyond MMP resulted in an additional oil recovery. A kinetically slow and peripheral vaporizing gas drive was denoted as the primary recovery mechanism for CO₂ huff-n-puff. While an effective injection pressure of 200 psi higher than MMP was identified as the upper limit of soaking pressure, which was caused by the pressure drop from shale core surface to the central region (Li et al., 2017). Gamadi et al. (2014) and Elwegaa et al. (2019) studied the performance of cyclic CO₂-EOR in shale formation as well as the influences of various factors, such as soaking pressure, soaking cycle, and temperature on shale oil recovery. However, to date, the prevalent literature investigated CO₂-EOR performance from a macroscopic core scale, and more works should be conducted to investigate the microscopic oil recovery characteristics from different types of pores in shale.

Unlike conventional reservoirs, a heterogeneous pore system is usually presented in shale reservoirs including small organic pores (OPs) with an average pore size below 10 nm that develop in kerogen due to thermal maturation and large inorganic pores (IPs) with multi-scale pore size formed by inter- and intraparticle pores and microfractures develop in the matrix (Cudjoe et al., 2021; Kang et al., 2011). Shale oil is normally trapped in kerogen, OPs, and IPs in the forms of free, adsorbed, and adsorbed states, resulting in much more complex flow behavior for CO₂ huff-n-puff process (Bustin and Bustin, 2012; Chen et al., 2011). NMR spectroscopy is considered a fast, precise, and nonintrusive tool to explore shale oil distribution within different types of pores after oil saturation and CO₂ huff-n-puff process since it can measure hydrogen-bearing fluid at pore scale. In a typical NMR measurement, hydrogen nuclei signals resulting from the interaction of magnetic spins of hydrogen nuclei with external magnetic fields are detected, and then the hydrogen-bearing fluid distributions are computed from the signal intensity curve as a function of relaxation time (Bloembergen et al., 1948). In the field of petroleum development, two types of NMR spectra have been widely used, named T_2 and T_1 - T_2 spectra. The longitudinal relaxation time T_1 reflects the ability of the object to transmit energy to its surroundings, and the transverse relaxation time T_2 reflects fluid mobility (Liu et al., 2020). Gong et al. (2022) investigated the effects of kerogen on the EOR performance of CO₂ flooding by comparing the differences in T_2 NMR spectra of shale samples before and after experiments. Zhu et al. (2019) examined microscopic CO₂ miscible flooding process in shale from pore scale using T_2 NMR technique. Wang et al. (2020) determined the pore size of mobile shale oil induced by CO₂ huff-n-puff by T_2 relaxation time. However, due to the limitation of T_2 NMR spectrum in accurately differentiating fluids with similar T_2 relaxation time, NMR signals from different fluids may overlap on T_2 NMR spectrum (Zhang et al., 2021).

Recent research mainly focuses on distinguishing various fluids co-existing in the complex shale pore system using T_1 - T_2 NMR spectrum (Fleury and Romero-Sarmiento, 2016; Yan et al., 2017; Zhang et al., 2020). For example, Cudjoe et al. (2021) evaluated the saturation of shale cores and CO₂ huff-n-puff process using this method. Dang (2019) investigated the fundamental drive of CO₂ huff-n-puff in promoting shale oil recovery. The influences of various factors on shale oil recovery such as soaking pressure, core size, and permeability were also investigated using T_1 - T_2 NMR spectrum (Cruz et al., 2022; Kumar et al., 2020). Owing to the superior accuracy of this spectrum in identifying hydrogen-bearing fluids, the extracting process of shale oil residing in different types of pores induced by the injected CO₂ can be clearly revealed if the experiments are rigorously designed and performed (Dang, 2019).

Herein, we employed T_1 - T_2 NMR spectroscopy to evaluate the oil saturation process of shale cores to optimize this scheme, and then performed CO₂ huff-n-puff on these well-saturated cores. The CO₂ huff-n-puff process was monitored online to figure out the influences of soaking pressure and cycles on shale oil recovery from different types of pores. To simplify the operation, connate water was not created and three typical soaking pressures (below MMP, near MMP, and above MMP) were selected for experiments. The results of this study can deepen the intuitionistic understanding of CO₂ huff-n-puff in extracting shale oil from different types of pores and provide some new insights into oil recovery mechanisms in shale.

2. Experimental sections

2.1. Materials

Homogenous outcrop core samples were outcrops collected from the 7th Member of the Yanchang Formation. The basic petrophysical properties of these core samples are listed in Table 1. The porosity and permeability of the core plugs were measured by helium saturation and helium pressure-pulse-decay methods, respectively. The core samples showed porosity of 3.65%–4.03% and permeability of 0.00224–0.00365 mD. All the plugs demonstrated similar porosity and permeability. Table 2 shows the mineralogy of the shale core samples analyzed using an X-ray diffractometer. Fig. 1 shows the general pore structure of the shale core samples, and IPs, OPs, and kerogen could be observed as labeled on the SEM images. Dead shale oil from the Changqing Oilfield, with a density of 0.75 cm³/g and a viscosity of 3.72 mPa s at room temperature, was used in this work.

2.2. Experimental setup and procedures

2.2.1. Determination of MMP between CO₂ and crude oil

MMP is one of the crucial parameters for gas injection. To investigate the impact of different soaking pressures on shale oil recovery after CO₂ huff-n-puff, MMP between CO₂ and crude oil was initially determined at reservoir temperature using the vanishing interfacial tension (VIT) method as shown in Fig. 2. The measurement accuracy was $\pm 10\%$. By extrapolating the IFT curve to the intersection with the x -axis, the multi-contact MMP was estimated to be 14.0 MPa. The VIT method could significantly reduce experimental time while maintaining a high accuracy (Ayirala, 2011; Hawthorne et al., 2016).

2.2.2. Core saturation

The oil saturation process of shale core samples was very slow, while some studies have claimed that the saturation process only took 2–3 days. This might not be sufficient due to the hindered

Table 1
Petrophysical properties of the core samples.

Core sample	Porosity, %	Permeability, mD	TOC, %	Diameter, cm	Length, cm
CQ-1	4.03	0.00224	2.27	2.49	6.82
CQ-2	3.75	0.00365	2.38	2.50	6.73
CQ-3	3.65	0.00290	2.32	2.49	6.81

Table 2
Mineralogy of the core samples from the X-ray diffraction analysis.

Core sample	Mineral composition, wt%						Total, wt%
	Quartz	K-feldspar	Plagioclase feldspar	Calcite	Pyrite	Total clay	
CQ-1	25.8	7.0	9.3	3.2	16.0	38.4	99.7
CQ-2	30.5	8.3	11.0	4.2	11.8	34.3	100.1
CQ-3	28.8	7.9	11.5	4.7	11.2	35.9	100.0

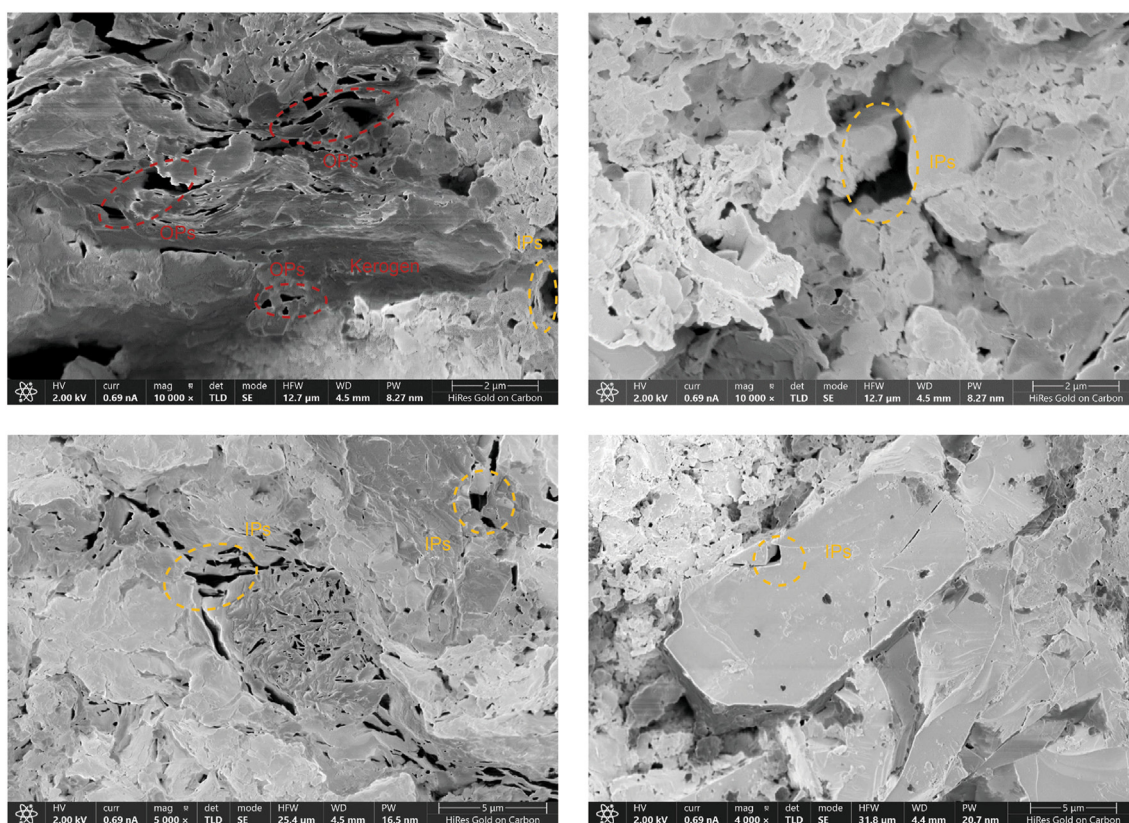


Fig. 1. DB-SEM images of the core samples.

mass transfer process in tiny pores (Chen et al., 2024). Since there is no standard procedure for saturating shale core samples, an effective saturation method was established based on the published literature and our experiences. The experimental setup for oil saturation is shown in Fig. 3. The maximum temperature and pressure resistance of the setup were 120 °C and 32 MPa, respectively. There was a fine mesh screen at the end cap of the saturation apparatus, which ensured that during the saturation process, the bottom of the core sample could fully contact with crude oil.

Before saturation, all the core plugs were dried at 115 °C until the weight of the core samples remained unchanged. The core plugs were then placed one at a time in the setup, as shown in Fig. 4. The setup was vacuumed for 2 days to remove any gas impurities in the core samples and pipelines, and then pressurized

with crude oil to 30 MPa. The core plug was removed from the saturation setup and weighed using a high-precision electronic balance every 4 days until the weight difference between two consecutive measurements was less than 0.001 g. The core samples before and after saturation were also subjected to an NMR spectrometer to obtain their T_1 – T_2 NMR spectra.

2.2.3. CO₂ puff-n-puff experiments

To investigate the dynamic distribution changes of crude oil in OPs and IPs during CO₂ huff-n-puff, while minimizing the adverse effects of temperature and pressure changes, the huff-n-puff experiments were conducted in an NMR spectrometer, as shown in Fig. 5. The experiments were monitored online throughout all the phases. The permanent magnet of the NMR apparatus

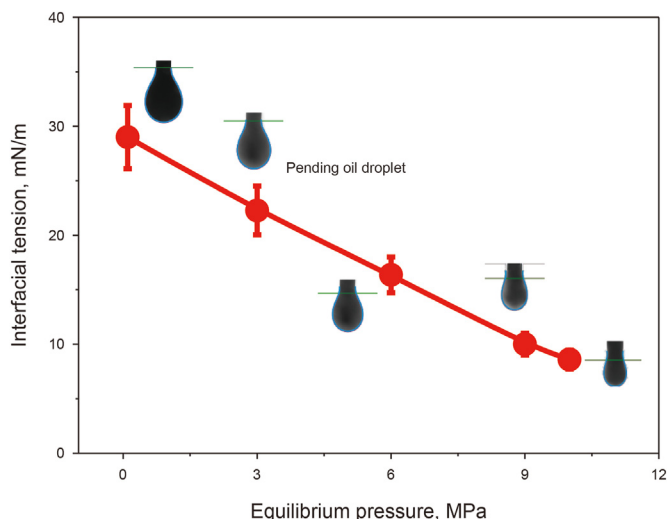


Fig. 2. The measured IFT between CO₂ and crude oil vs. equilibrium pressure.

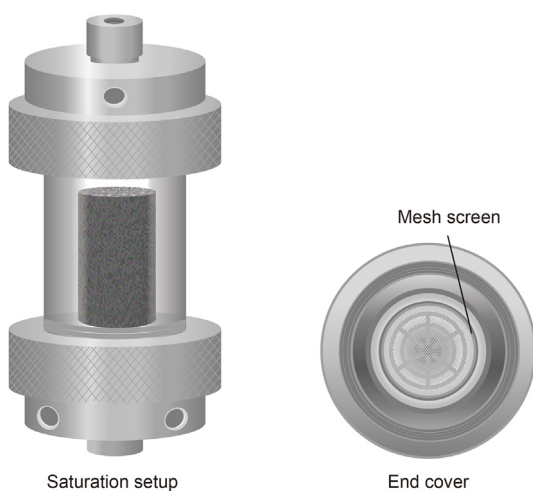


Fig. 3. The schematic diagram of the high-temperature and high-pressure saturation setup.

(MacroMR12-150 HTHP-I, Suzhou Niumag Analytical Instrument Corp., China) has a strength of 0.3 ± 0.05 T with a resonance frequency of 12 MHz. Echo spacing and waiting time are 0.1 ms and

2000 ms, respectively. The echo and scanning numbers are 4096 and 64, respectively.

The core plug was wrapped with heat shrink tubing before being placed into the core container to reduce the contact area between CO₂ and the core sample. A confining pressure was then applied by fluorocarbon oil until it exceeded the soaking pressure by 1–2 MPa. Since fluorocarbon oil was free of hydrogen nuclei, only hydrogen-bearing fluids resided in the core samples were NMR visible. Subsequently, CO₂ was injected into the core container until the soaking pressure was reached, after which the T₁–T₂ NMR spectrum of the core plug was measured. After a soaking duration of 3 h, the core container was depressurized at a rough rate of 0.1 MPa/min to a back pressure. The back pressure was kept constant at 6.8 MPa throughout the whole process to simulate the typical bottomhole pressure of production wells in unconventional reservoirs after primary depletion (Alzobaidi et al., 2022).

3. Results and discussion

3.1. The characteristics of shale oil distribution after saturation

Since high pressure contributes to the saturation performance of shale core samples, the core container was pressurized to 30 MPa to accelerate this process while preventing core fracturing (Gamadi et al., 2014). The saturation results are shown in Figs. 6 and 7. All the core plugs followed a similar saturation pattern with respect to oil volume and saturation in percentage almost 70% of oil was saturated into the core samples within the first 4 days, and then the incremental oil volume decreased rapidly. After 16 days, the saturated oil volume remained almost unchanged, and the oil saturation reached a highest magnitude of 46.2% after 20 days. The abovementioned saturation trend conformed to the characteristics of oil migration in shale. During the initial saturation process, crude oil rapidly migrated into the large pores at the core surface, primarily controlled by external pressure. Subsequently, due to the tight matrix of the shale core, the impact of external pressure on the inward migration of the saturated oil into the matrix diminished. As a result, the transport of crude oil towards the deeper regions of the core was mainly governed by molecular diffusion driven by concentration gradients, causing a deceleration in the migration rate of the crude oil. Therefore, a vacuum and pressurizing procedure with a duration of at least 16 days was highly recommended for oil saturation in such core samples, as we summarized before (Chen et al., 2024). Note that to avoid any damages to the core plugs, a maximum pressure of 30 MPa was used to saturate the plugs and the oil saturation reached only 46.2% after 20 days.

With the assistance of an NMR spectrometer, the T₁–T₂ NMR

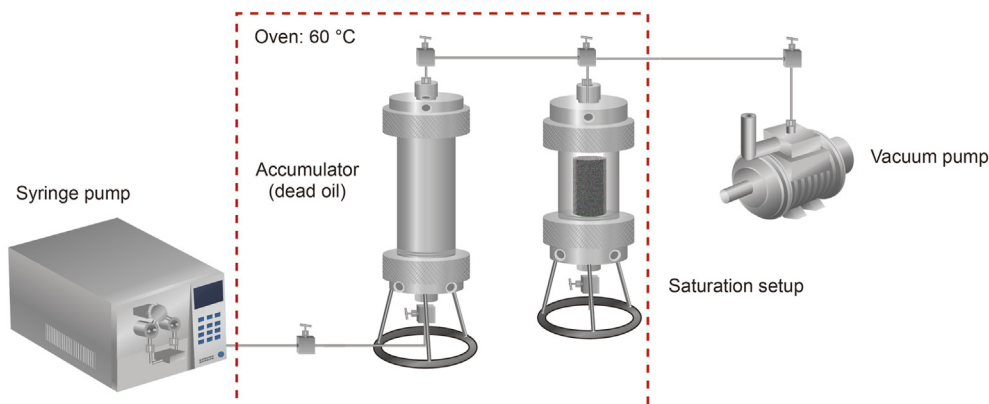


Fig. 4. The schematic diagram of the saturation setup.

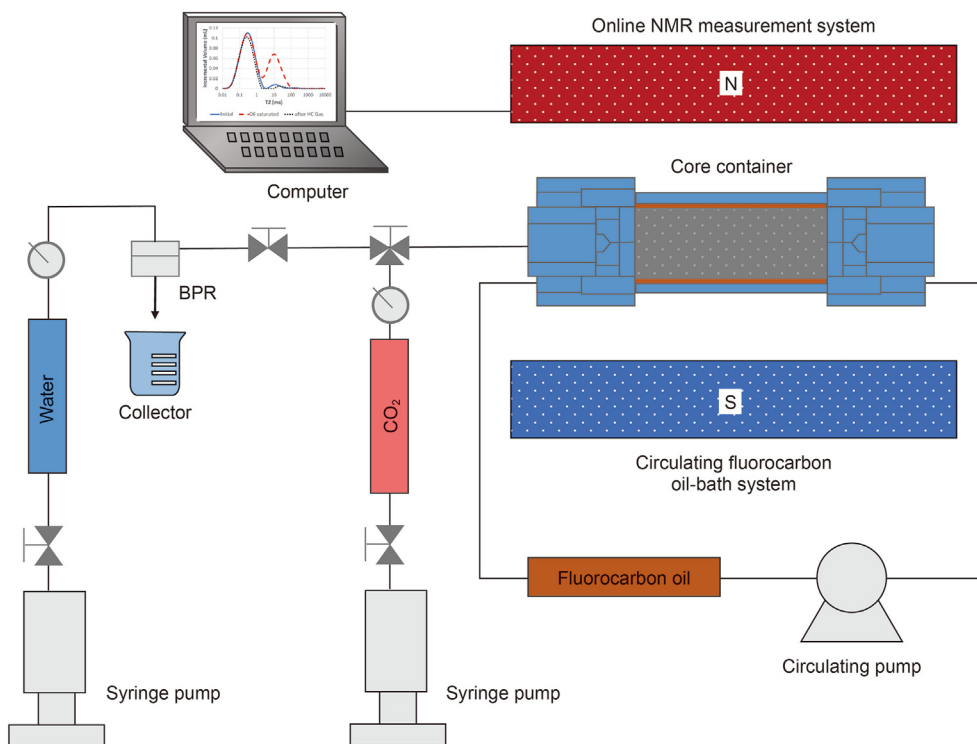


Fig. 5. The schematic diagram of the CO₂ huff-n-puff experiment.

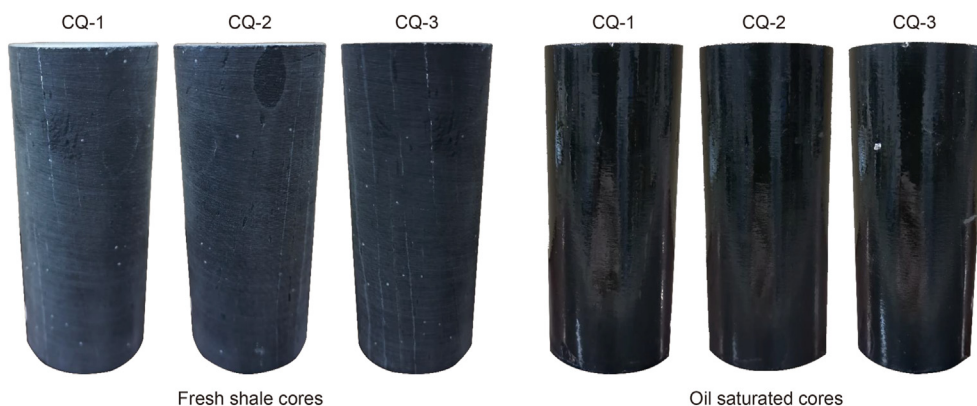


Fig. 6. Shale core plugs before and after oil saturation.

spectra could be readily obtained as shown in Fig. 8, in which three distinct regions were observed for all the samples. As reported, these regions could be assigned to kerogen, oil in OPs, and oil in IPs, respectively (Li et al., 2018; Zhang et al., 2020; Cudjoe et al., 2021). It was noted that the NMR signals of kerogen significantly increased after saturation, which was attributed to the fact that the oil-wet organic pore walls formed by kerogen have a strong adsorption affinity to crude oil, leading the NMR signals of the adsorbed oil in OPs to overlap with the original NMR signals of kerogen. Moreover, kerogen could dissolve and absorb saturated oil, thereby further enhancing the NMR signals of this region.

3.2. The production characteristics of shale oil trapped in different types of pores during CO₂ huff-n-puff blow MMP

The T_1 – T_2 NMR spectra of CQ-1 core sample before and after CO₂ huff-n-puff at a soaking pressure of 11.0 MPa (< MMP) are

shown in Fig. 9. As seen, the NMR signals of kerogen and OPs were hardly changed even after three cycles were performed, indicating a fact that the oil resided here was not extracted by CO₂. In contrast, the oil in IPs was slightly mobilized. It could be inferred that under immiscible conditions, the limited diffusion capability of CO₂ and also the weak interaction with crude oil hindered the migration of the saturated oil from kerogen and OPs. Only a small fraction of the readily accessible oil trapped in IPs was extracted during the first and second cycles, leading to an insignificant oil extraction in shale.

By integrating the NMR signals of various regions on the T_1 – T_2 NMR spectra, the oil extraction from different pores could be further quantitatively analyzed as shown in Fig. 10. It was found that the cumulative oil recovery (COR) from total pores after three cycles was merely 14.1% OOIP, among which the COR of the first cycle was 7.93% OOIP, accounting for more than half COR after three cycles. However, the oil recovery rapidly dropped with cycles, which produced an oil recovery of 4.78% OOIP in the second cycle

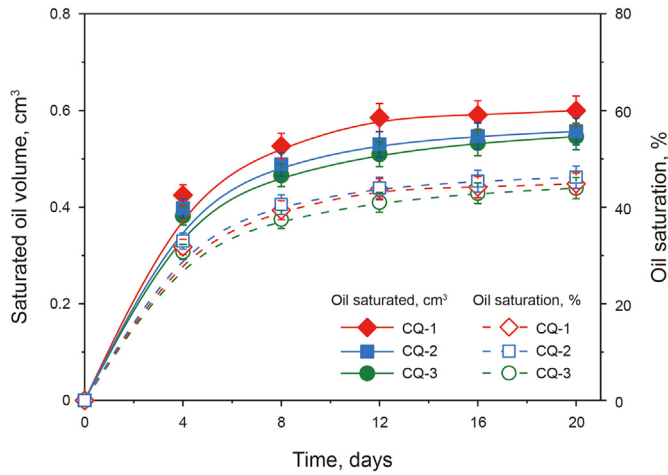


Fig. 7. Saturated oil volume and saturation vs. time.

and 1.39% OOIP in the third cycle, suggesting that CO₂ huff-n-puff was insufficient to extract shale oil from the third cycle. In addition, the oil recoveries from IPs in the first, second, and third cycles accounted for 24.67%, 11.63%, and 5.68% OOIP, respectively. Nevertheless, the shale oil trapped in OPs was barely recovered, resulting

in oil recoveries of only 5.65%, 3.85%, and 0.79% OOIP in three cycles, respectively. Besides, the shale oil extracted from OPs was mainly derived from the free oil in OPs, corresponding to the change in NMR signals in the OPs region, while the oil adsorbed on the organic pore walls and kerogen was hardly produced, as indicated in Fig. 9. It could be generally concluded that IPs was the primary target of CO₂ huff-n-puff in shale.

3.3. The production characteristics of shale oil trapped in different types of pores during CO₂ huff-n-puff at MMP

With the increase of the soaking pressure to MMP, significant NMR signal changes were readily observed on the T₁–T₂ NMR spectra before and after CO₂ huff-n-puff at a pressure of 14.0 MP (MMP), as shown in Fig. 11. Similar to the results in Fig. 9, the NMR signals of IPs exhibited the most pronounced changes, followed by OPs and kerogen. Compared to the performance at immiscible conditions, the oil extracted from IPs and OPs was all significantly promoted.

As indicated in Fig. 12, the COR reached 26.01% OOIP after three cycles, among which the first cycle produced as high as 13.36% OOIP, which was mainly attributed to the further production of the oil in IPs. Compared to the results in Fig. 10, we can see that the oil recoveries of IPs increased from 24.67% to 32.07% OOIP after the first cycle when the soaking pressure was increased to MMP, and the oil recoveries of OPs also increased from 5.65% to 9.45% OOIP

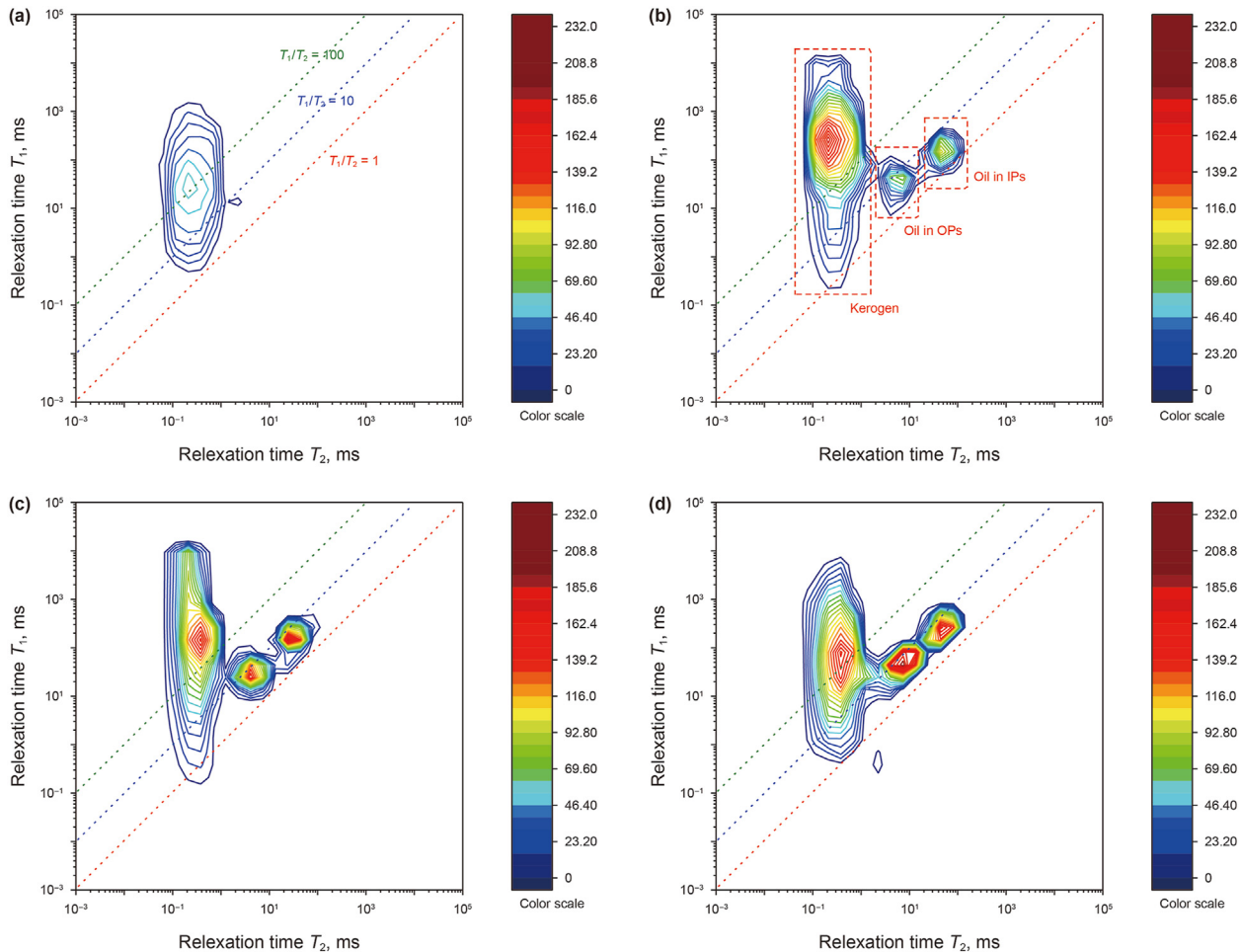


Fig. 8. T₁–T₂ NMR spectra of the core samples before and after saturation. (a) Spectrum of CQ-1 core sample before saturation. Spectra of CQ-1 (b), CQ-2 (c), and CQ-3 (d) core samples after saturation, respectively.

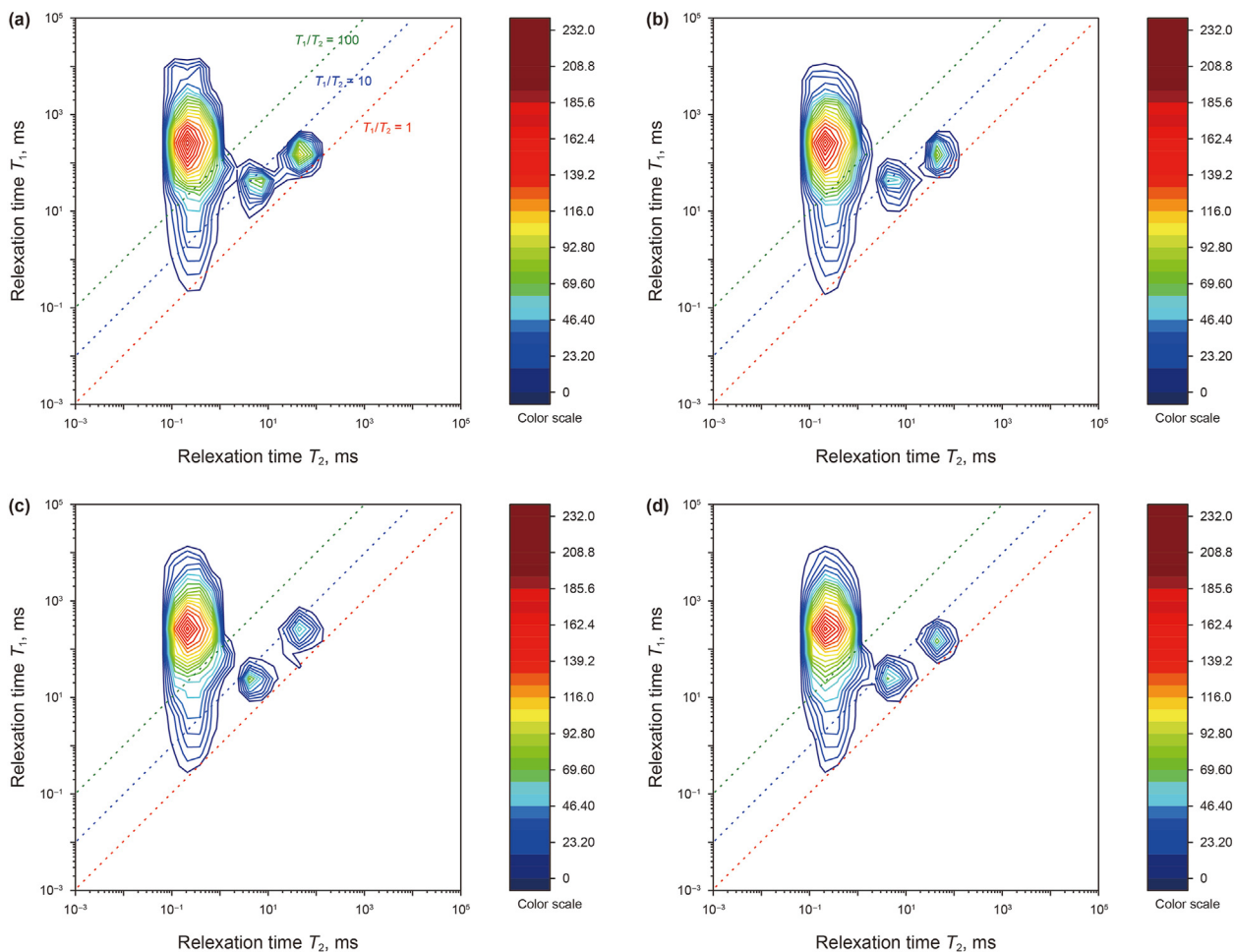


Fig. 9. T_1 – T_2 NMR spectra of immiscible CO_2 huff-n-puff on CQ-1 core sample after saturation (a), the first cycle (b), second cycle (c), and third cycle (d).

(Fig. 11). Apart from the first cycle, quite analogous changes also occurred for the second cycle and third cycle, which increased the oil recovery by 6.97% and 5.68% OOIP, respectively. However, the incremental oil recoveries of IPs for the second cycle and third cycle were insignificant, merely 8.96% and 9.92% OOIP, respectively.

In summary, the oil recovery of miscible CO_2 huff-n-puff significantly increased compared to immiscible process, and the first cycle contributed the majority of oil production, which

accounted for 51.36% OOIP of the COR after three cycles. The oil production from OPs and IPs both increased substantially, with CORs of 20.77% and 50.95% OOIP, respectively.

3.4. The production characteristics of shale oil trapped in different types of pores during CO_2 huff-n-puff at above MMP

When the soaking pressure was further increased to a

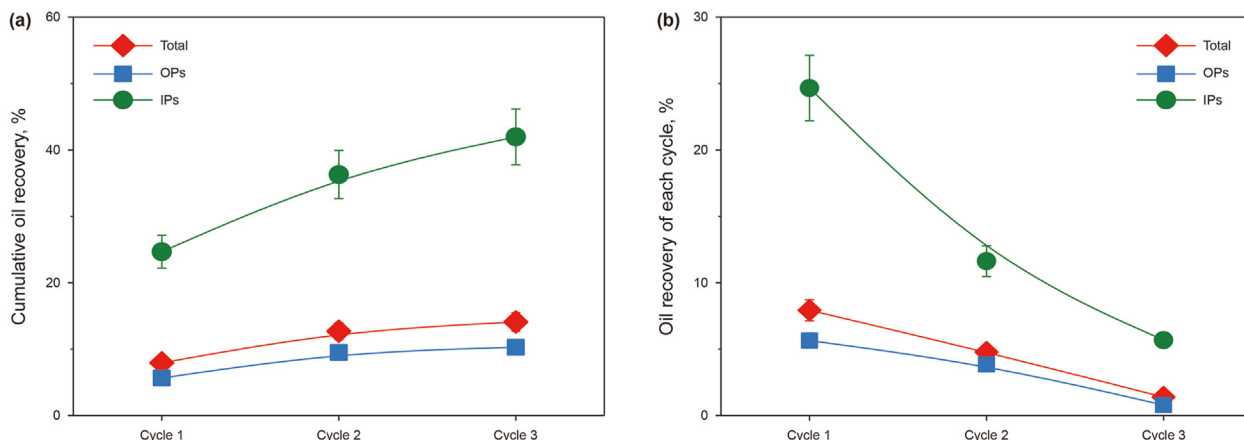


Fig. 10. Oil extraction performance of immiscible CO_2 huff-n-puff vs. cycles on CQ-1 core sample.

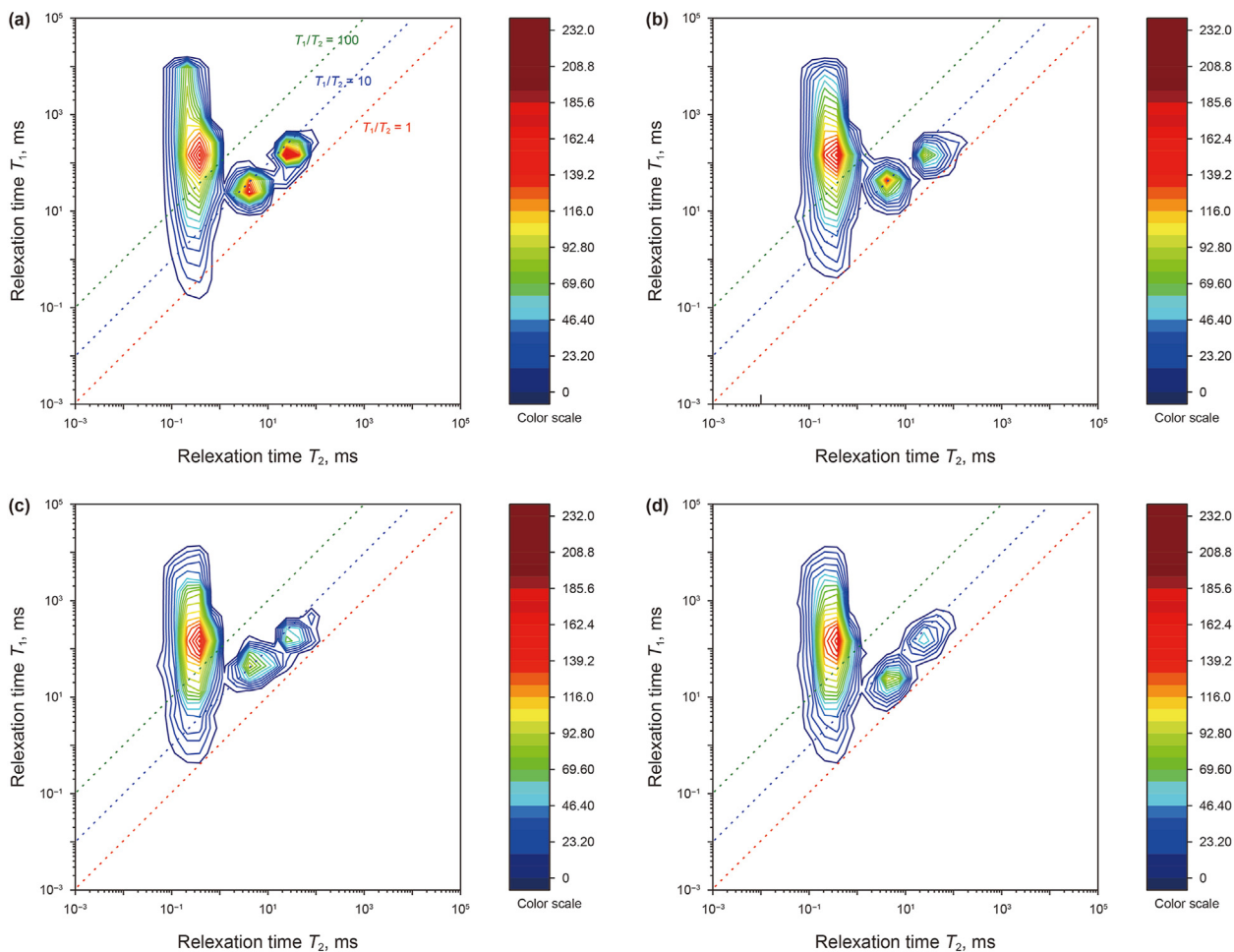


Fig. 11. T_1 – T_2 NMR spectra of immiscible CO₂ huff-n-puff on CQ-2 core sample after saturation (a), the first cycle (b), second cycle (c), and third cycle (d).

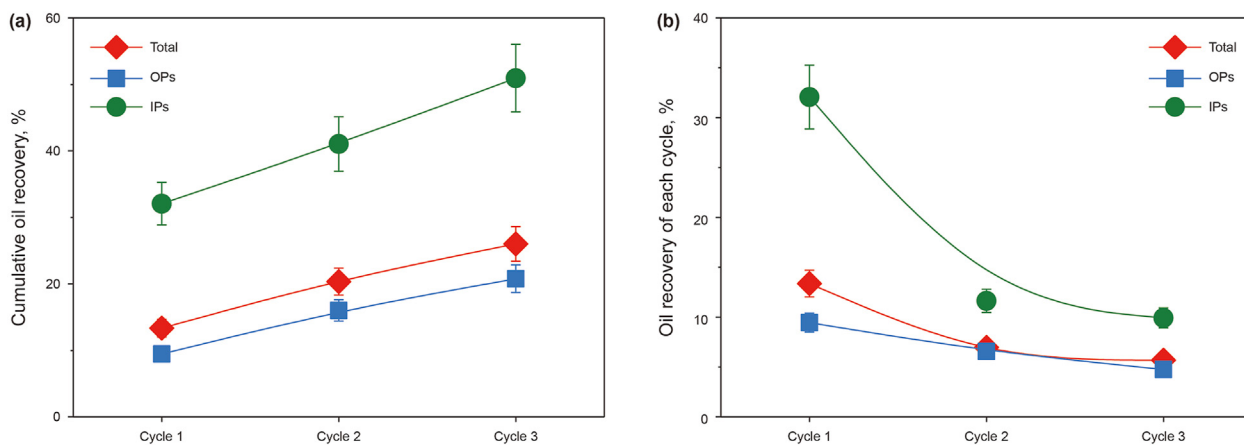


Fig. 12. Oil extraction performance of miscible CO₂ huff-n-puff vs. cycles on CQ-2 core sample.

magnitude that significantly exceeded MMP, the COR induced by CO₂ huff-n-puff could be further promoted. Based on the T_1 – T_2 NMR spectra of CQ-3 core sample, as shown in Fig. 13, the NMR signals of three regions further decreased with the increase of soaking pressure, particularly in the IPs region. The NMR signals of the OPs and kerogen regions also significantly decreased in the first two cycles, indicating that increasing soaking pressure to

significantly exceed MMP not only promoted the mobilization of the shale oil trapped in IPs, but also increased the oil production from OPs.

Fig. 14 summarizes the oil extraction performance of CO₂ huff-n-puff process in the shale core sample at an above miscible pressure of 17.0 MPa. Compared to the results at the immiscible condition and miscible condition, when the pressure was increased further

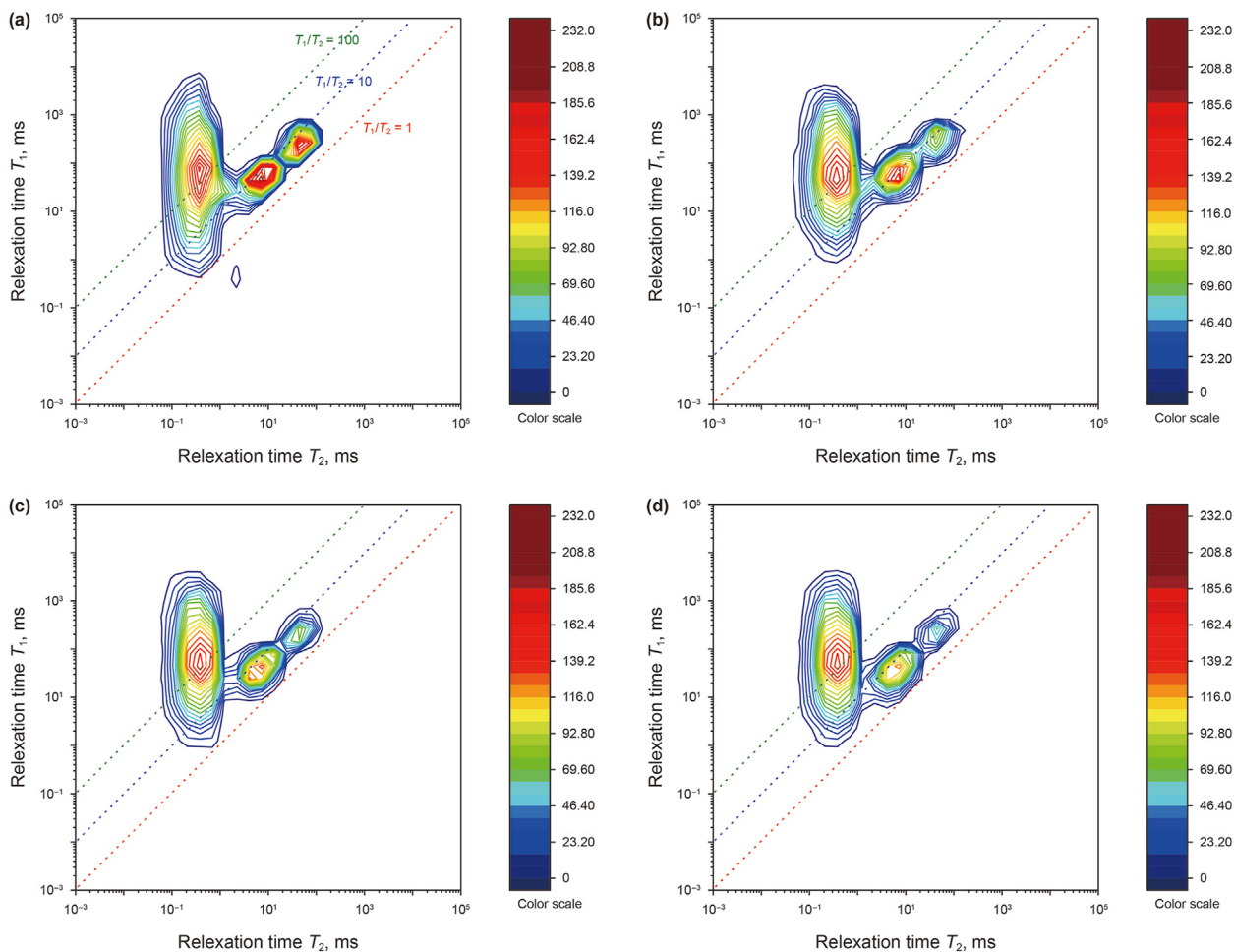


Fig. 13. T_1 – T_2 NMR spectra of above-miscible CO_2 huff-n-puff on CQ-3 core sample after saturation (a), the first cycle (b), second cycle (c), and third cycle (d).

exceeding MMP, the COR after three cycles achieved 30.19% OOIP, while the oil recovery of IPs reached 70.04% OOIP, which was mainly induced by further CO_2 extraction of shale oil during the last two cycles, with oil recoveries of 18.68% and 13.76% OOIP, respectively. In contrast, despite the further increase of the oil recovery from OPs, the COR of OPs remained insignificant, with oil recoveries of 11.23%, 9.95%, and 3.04% OOIP in three cycles, respectively. In general, even when the pressure exceeded MMP, the COR still

increased with pressure, while the increment of oil recovery decreased gradually. This might be caused by the limited mass transfer in the nanosized shale pores as discussed below.

3.5. Effect of the huff-n-puff cycle on oil recovery from different types of pores

As indicated in Figs. 10, 12, and 14, the oil recovery of each cycle

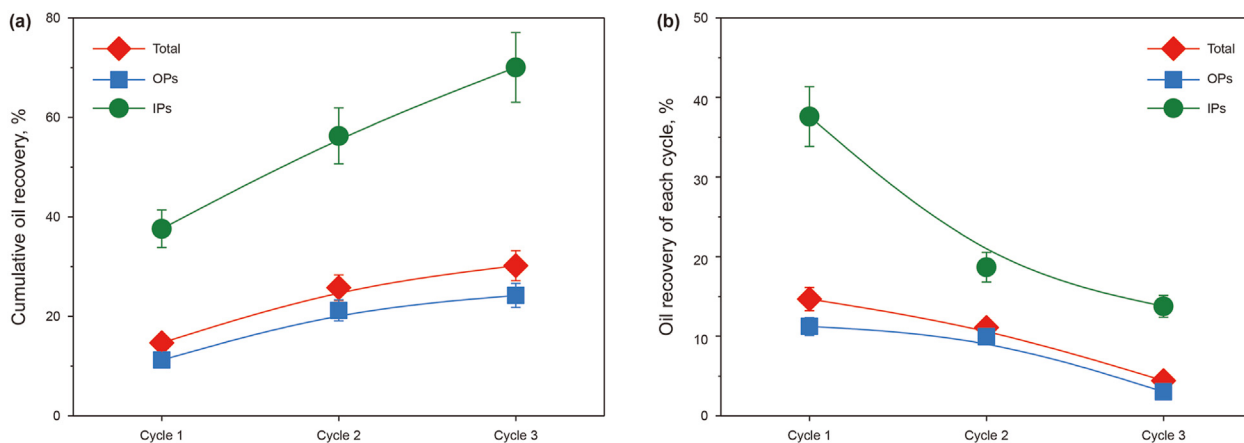


Fig. 14. Oil extraction performance of above-miscible CO_2 huff-n-puff vs. cycles on CQ-3 core sample.

steeply dropped with huff-n-puff cycles. In the first cycle, CO₂ penetrated the tight matrix and effectively extracted the oil mainly trapped in IPs near the surface. In the subsequent cycles, CO₂ needed to migrate further into deeper regions to interact with the oil in place. However, in the presence of nanosized pores, the influence of external pressure gradually diminished as the migration distance increased, and the migration of CO₂ towards the deep region of the matrix became dominated by molecular diffusion. Hindered by the slow diffusion and diluted concentration of CO₂ in the deep region, the interaction between CO₂ and oil was obstructed, resulting in a rapid decrease in oil production with cycles. Moreover, CO₂ preferentially diffused into the more accessible pores during the initial soaking period, resulting in the extraction of relatively easily producible oil in the first cycle. As a result, only a limited amount of remaining accessible oil was available for the subsequent cycles. To achieve a comparable oil recovery to that in the first cycle, it is necessary for CO₂ to extract more oil trapped in OPs and kerogen with a much lower mobility. Consequently, the oil recovery decreased significantly with cycles.

In conclusion, the easily accessible oil trapped in the large IPs near the surface was mainly extracted in the first huff-n-puff cycle, and CO₂ needed to further diffuse into the deeper region of the shale tight matrix in the second and third cycles, resulting in a significant decrease in oil recovery.

3.6. Effect of soaking pressure on oil recovery from different types of pores

For conventional reservoirs, the sweep efficiency of core flooding could be maximized to 100% when the injection pressure reaches MMP, which thus leads to the formation of a miscible front with no capillary pressure (Lake, 2010). However, due to the limited mass transfer caused by complex shale pore systems, CO₂ preferentially diffuses into accessible pores in the tight matrix from highly permeable fractures, and thus there is no significant miscible front formed during CO₂ huff-n-puff process, which consequently leads to different oil recovery performance with pressure increase. The relationship between COR and soaking pressure for different pores is shown in Fig. 15. COR demonstrated a monotonically increasing tendency with soaking pressure, even when the pressure noticeably exceeded MMP. We then conducted a linear fitting to the data, as represented by the solid lines. It was found that the slopes of the fitting line were very close. At immiscible conditions, CO₂ primarily migrated into large IPs. Due to the limited interaction between CO₂ and oil, only a small fraction of trapped oil with relatively high mobility in IPs was produced. The trapped oil in OPs was almost unaffected due to the strong adsorption affinity to the oil-wet surface. However, when the soaking pressure increased to MMP and significantly higher than MMP, the interaction between CO₂ and oil intensified, and the interfacial tension also diminished, resulting in an additional oil production in IPs. Besides, with the increase in soaking pressure, the dissolution/extraction capability of CO₂ was promoted, allowing it to overcome the confinement of the oil-wet surface in OPs and extract more oil during the soaking stage.

In conclusion, for shale oil reservoirs, the oil recovery continuously increased with the increase in CO₂ huff-n-puff pressure, but the incremental oil recovery steeply decreased with cycles, regardless of whether CO₂ and oil formed a miscible phase (i.e., whether the soaking pressure reached MMP). The impact of soaking pressure on oil recovery mainly lay in the fact that high pressure promoted CO₂ diffusion in tight shale matrix and CO₂ dissolution/extraction capability in the trapped oil (Hawthorne et al., 2017; Tovar et al., 2021). Consequently, the diffusion distance of CO₂ in the shale matrix expanded, the mobilization of the trapped oil in

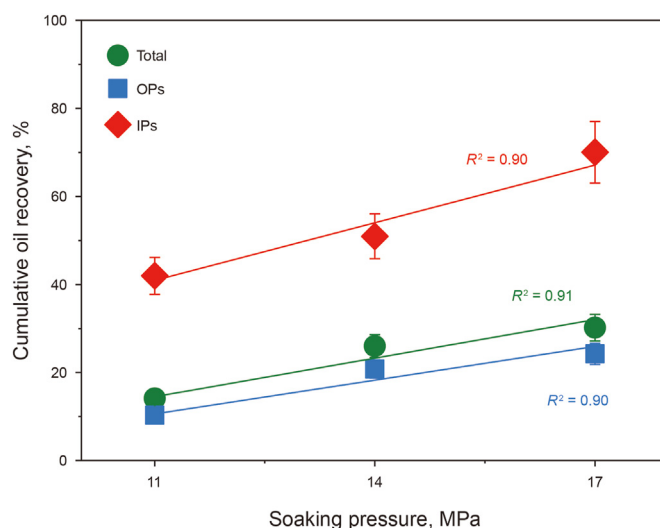


Fig. 15. COR of different pores vs. soaking pressure after CO₂ huff-n-puff.

different pores increased, and ultimately, the oil recovery after CO₂ huff-n-puff was improved.

4. Limitations of this study

We presented the following limitations that might cause an overestimation of the oil recovery compared with those of field cases.

- The oil used in this work was a degassed oil without very light components. This might affect CO₂–oil interactions, leading to a lower oil recovery.
- The volume ratio between CO₂ in the container and the oil in the core might be exaggerated to intensify the mass exchange and make this process detectable. This would lead to an overestimation of the oil recovery compared to realistic cases.
- The attention of this work was mainly placed on the experimental exploration of shale oil extraction from different types of pores. Numerical modeling and theoretical analysis were not included due to the complex flow behavior of multi-phase fluids in nanosized pores.

It is believed that the results of this study can deepen our understanding of CO₂ huff-n-puff in extracting shale oil from different types of pores and provide some new insights into oil recovery mechanisms in shale. More rigorous and comprehensive experiments are needed to solidify the observations of the oil recovery dynamics and mechanisms.

5. Conclusions

We designed and performed a series of CO₂ huff-n-puff experiments on shale core samples to explore the oil extraction dynamics from different types of pores. To accomplish this goal, online T₁–T₂ NMR spectroscopy was employed to monitor the events occurred at pore scale. Based on the data, the following conclusions can be generally drawn.

- (1) Three distinct NMR signal regions can be identified on the T₁–T₂ NMR spectra of the oil saturated core, corresponding to kerogen, OPs, and IPs regions.

- (2) The oil resided in IPs of shale core sample was the primary target of CO₂ huff-n-puff, while the oil trapped in OPs in an adsorbed state and oil absorbed in kerogen was hardly extracted except a small fraction of free oil in OPs.
- (3) The oil recovery quickly decreased with huff-n-puff cycles and most of the oil was produced in the first cycle as being extracted from both OPs and IPs. In the second cycle, the oil trapped in IPs was mainly produced. While minimal oil production was yielded in the third cycle for all the pores.
- (4) COR demonstrated a linear increase with pressure, even when the pressure significantly exceeded MMP, indicating that the formation of a miscible phase between CO₂ and oil was not the primary drive for CO₂ huff-n-puff in shale, but rather than the promotion of high pressure on CO₂ diffusion in shale matrix and CO₂ dissolution/extraction capability in the trapped oil.

CRediT authorship contribution statement

Yi-Jian Ren: Writing – original draft, Investigation. **Bing Wei:** Writing – review & editing, Supervision, Resources, Project administration, Funding acquisition, Conceptualization. **Bing-Xin Ji:** Writing – original draft, Investigation. **Wan-Fen Pu:** Writing – review & editing, Project administration. **Dian-Lin Wang:** Writing – review & editing, Supervision. **Jin-Yu Tang:** Writing – review & editing, Supervision. **Jun Lu:** Writing – review & editing.

Declaration of competing interest

The authors declare that there is no conflict of interest.

Acknowledgments

The authors gratefully acknowledge the financial support of National Key Research and Development Program of China (2023YFE0120700), National Natural Science Foundation of China (52274041), and Distinguished Young Sichuan Science Scholars (2023NSFSC1954). Jun Lu acknowledges the McDougall School of Petroleum Engineering at The University of Tulsa for the support of this research. The anonymous reviewers for their valuable comments are sincerely appreciated.

References

- Alzobaidi, S., Kortunov, P., Chhatre, S., et al., 2022. Experimental evaluation of huff and puff EOR mechanisms in unconventional rock. In: SPE/AAPG/SEG Unconventional Resources Technology Conference. <https://doi.org/10.15530/urtec-2022-3719062>.
- Ayrala, S.C., 2011. Comparative evaluation of a new gas/oil miscibility-determination technique. *J. Can. Petrol. Technol.* 50 (9), 71–81. <https://doi.org/10.2118/99606-PA>.
- Bloembergen, N., Purcell, E.M., Pound, R.V., 1948. Relaxation effects in nuclear magnetic resonance absorption. *Phys. Rev.* 73 (7), 679. <https://doi.org/10.1103/PhysRev.73.679>.
- Bustin, A.M., Bustin, R.M., 2012. Importance of rock properties on the producibility of gas shales. *Int. J. Coal Geol.* 103, 132–147. <https://doi.org/10.1016/j.coal.2012.04.012>.
- Chen, H., Ji, B., Wei, B., et al., 2024. Experimental simulation of enhanced oil recovery on shale rocks using gas injection from material to characterization: Challenges and solutions. *Fuel* 356, 129588. <https://doi.org/10.1016/j.fuel.2023.129588>.
- Chen, S., Zhu, Y., Wang, H., et al., 2011. Shale gas reservoir characterisation: A typical case in the southern Sichuan Basin of China. *Energy* 36 (11), 6609–6616. <https://doi.org/10.1016/j.energy.2011.09.001>.
- Cruz, F., Mamoudou, S., Tinni, A., 2022. The impact of gas-oil miscibility on oil recovery during huff-and-puff eor in organic-rich shales. In: SPE Annual Technical Conference and Exhibition. <https://doi.org/10.2118/210028-MS>.
- Cudjoe, S.E., Barati, R., Tsau, J.-S., et al., 2021. Assessing the efficiency of saturating

- shale oil cores and evaluating hydrocarbon gas huff 'n' puff using nuclear magnetic resonance. *SPE Reservoir Eval. Eng.* 24 (2), 429–439. <https://doi.org/10.2118/205027-PA>.
- Dang, S., 2019. Understanding the Fundamental Drive Mechanisms for Huff-N-Puff Enhanced Oil Recovery in Tight Formations. Ph.D. Dissertation. University of Oklahoma.
- Elwegaa, K., Emadi, H., Soliman, M., et al., 2019. Improving oil recovery from shale oil reservoirs using cyclic cold carbon dioxide injection—An experimental study. *Fuel* 254, 115586. <https://doi.org/10.1016/j.fuel.2019.05.169>.
- Fakher, S., El-Tonbary, A., Abdelaal, H., et al., 2020. Increasing oil recovery from unconventional shale reservoirs using cyclic carbon dioxide injection. In: SPE Europec. <https://doi.org/10.2118/200636-MS>.
- Fleury, M., Romero-Sarmiento, M., 2016. Characterization of shales using T₁–T₂ NMR maps. *J. Petrol. Sci. Eng.* 137, 55–62. <https://doi.org/10.1016/j.petrol.2015.11.006>.
- Gamadi, T.D., Sheng, J.J., Soliman, M.Y., et al., 2014. An experimental study of cyclic CO₂ injection to improve shale oil recovery. In: SPE Improved Oil Recovery Symposium. <https://doi.org/10.2118/169142-MS>.
- Gong, H., Zhang, H., Lv, W., et al., 2022. Effects of kerogen on the flow and EOR performance of oil in shale cores during CO₂ flooding process investigated by NMR technology. *SPE J.* 27 (4), 2244–2256. <https://doi.org/10.2118/209581-PA>.
- Hawthorne, S.B., Gorecki, C.D., Sorensen, J.A., 2013. Hydrocarbon mobilization mechanisms from upper, middle, and lower Bakken reservoir rocks exposed to CO₂. In: SPE Unconventional Resources Conference Canada. <https://doi.org/10.2118/167200-MS>.
- Hawthorne, S.B., Miller, D.J., Jin, L., et al., 2016. Rapid and simple capillary-rise/vanishing interfacial tension method to determine crude oil minimum miscibility pressure: Pure and mixed CO₂, methane, and ethane. *Energy & Fuels* 30 (8), 6365–6372. <https://doi.org/10.1021/acs.energyfuels.6b01151>.
- Hawthorne, S.B., Miller, D.J., Grabanski, C.B., et al., 2017. Measured crude oil mmps with pure and mixed CO₂, methane, and ethane, and their relevance to enhanced oil recovery from middle Bakken and Bakken shales. In: SPE Unconventional Resources Conference. <https://doi.org/10.2118/185072-MS>.
- Hoffman, B.T., Rutledge, J.M., 2019. Mechanisms for huff-n-puff cyclic gas injection into unconventional reservoirs. In: SPE Oklahoma City Oil and Gas Symposium. <https://doi.org/10.2118/195223-MS>.
- Kang, S.M.M., Fathi, E., Ambrose, R.J.J., et al., 2011. Carbon dioxide storage capacity of organic-rich shales. *SPE J.* 16 (4), 842–855. <https://doi.org/10.2118/134583-PA>.
- Kumar, R., Ali, S.J., Mathur, A., 2020. A rigorous workflow for evaluation of huff and puff recovery efficiency of immiscible and miscible gases in unconventional reservoirs by integrating core tests with NMR and GC analysis. In: SPE/AAPG/SEG Unconventional Resources Technology Conference. <https://doi.org/10.15530/urtec-2020-3332>.
- Lake, L.W., 2010. Enhanced Oil Recovery. Society of Petroleum Engineers, Richardson, Texas, USA.
- Li, J., Huang, W., Lu, S., et al., 2018. Nuclear magnetic resonance T₁–T₂ map division method for hydrogen-bearing components in continental shale. *Energy & Fuels* 32 (9), 9043–9054. <https://doi.org/10.1021/acs.energyfuels.8b01541>.
- Li, L., Zhang, Y., Sheng, J., 2017. Effect of the injection pressure on enhancing oil recovery in shale cores during the CO₂ huff-n-puff process when it is above and below the minimum miscibility pressure. *Energy & Fuels* 31 (4), 3856–3867. <https://doi.org/10.1021/acs.energyfuels.7b00031>.
- Li, L., Wang, C., Li, D., et al., 2019. Experimental investigation of shale oil recovery from Qianjiang core samples by the CO₂ huff-n-puff EOR method. *RSC Adv.* 9 (49), 28857–28869. <https://doi.org/10.1039/c9ra05347f>.
- Liu, Z., Liu, D., Cai, Y., et al., 2020. Application of nuclear magnetic resonance (NMR) in coalbed methane and shale reservoirs: A review. *Int. J. Coal Geol.* 218, 103261. <https://doi.org/10.1016/j.coal.2019.103261>.
- Perez, F., Devegowda, D., 2020. A molecular dynamics study of soaking during enhanced oil recovery in shale organic pores. *SPE J.* 25 (2), 832–841. <https://doi.org/10.2118/199879-PA>.
- Tovar, F.D., Barrufet, M.A., Schechter, D.S., 2021. Enhanced oil recovery in the wolfcamp shale by carbon dioxide or nitrogen injection: an experimental investigation. *SPE J.* 26 (1), 515–537. <https://doi.org/10.2118/204230-PA>.
- Wang, H., Lun, Z., Lv, C., et al., 2020. Nuclear-magnetic-resonance study on oil mobilization in shale exposed to CO₂. *SPE J.* 25 (1), 432–439. <https://doi.org/10.2118/190185-PA>.
- Yan, W., Sun, J., Cheng, Z., et al., 2017. Petrophysical characterization of tight oil formations using 1D and 2D NMR. *Fuel* 206, 89–98. <https://doi.org/10.1016/j.fuel.2017.05.098>.
- Zhang, P., Lu, S., Li, J., et al., 2020. 1D and 2D nuclear magnetic resonance (NMR) relaxation behaviors of protons in clay, kerogen and oil-bearing shale rocks. *Mar. Petrol. Geol.* 114, 104210. <https://doi.org/10.1016/j.marpetgeo.2019.104210>.
- Zhang, X., Wei, B., You, J., et al., 2021. Characterizing pore-level oil mobilization processes in unconventional reservoirs assisted by state-of-the-art nuclear magnetic resonance technique. *Energy* 236, 121549. <https://doi.org/10.1016/j.energy.2021.121549>.
- Zhu, C., Sheng, J., Ettehadtavakkol, A., et al., 2019. Numerical and experimental study of enhanced shale-oil recovery by CO₂ miscible Displacement with NMR. *Energy & Fuels* 34 (2), 1524–1536. <https://doi.org/10.1021/acs.energyfuels.9b03613>.